

****Volume Title****

*ASP Conference Series, Vol. **Volume Number***

****Author****

© ****Copyright Year**** *Astronomical Society of the Pacific*

Kiloparsec-Scale Simulations of Magnetised Molecular Clouds in Disk Galaxies.

Sven Van Loo,¹ Michael J. Butler,² Jonathan C. Tan,² and Sam A. E. G. Falle³

¹*Harvard-Smithsonian Center for Astrophysics, 60 Garden Street, Cambridge, MA 02138, USA*

²*Department of Astronomy, University of Florida, Gainesville, FL 32611, USA*

³*Department of Applied Mathematics, University of Leeds, Woodhouse Lane, Leeds, LS2 9JT, UK*

Abstract. We present simulations of the evolution of self-gravitating dense gas on kiloparsec-size scales in a galactic disk, designed to study dense clump formation from giant molecular clouds (GMCs). These dense clumps are expected to be the precursors to star clusters and this process may be the rate limiting step controlling star formation rates in galactic systems as described by the Kennicutt-Schmidt relation. The evolution of these simulated GMCs and clumps is determined by self-gravity balanced by turbulent pressure support and the large scale galactic shear. While the cloud structures and densities significantly change during their evolution, they remain roughly in virial equilibrium for time scales exceeding the free-fall time of GMCs, indicating that energy from the galactic shear continuously cascades down. We implement star formation at a slow, inefficient rate of 2% per local free-fall time, but this still yields global star formation rates that are \sim two orders of magnitude larger than the observed Kennicutt-Schmidt relation due to the over-production of dense clump gas. To explain this discrepancy, we anticipate magnetic fields to provide additional support. Low-resolution simulations indeed show that the magnetic field reduces the star formation rate.

1. Introduction

Star formation in galaxies involves a vast range of length and time scales, from the tens of kiloparsec diameters and $\sim 10^8$ yr orbits of galactic disks to the ~ 0.1 pc sizes and $\sim 10^5$ yr dynamical times of individual prestellar cores (PSCs) (see McKee & Ostriker 2007, for a review). The interstellar medium (ISM) contains various forms of pressure support (including thermal, magnetic and turbulent), large-scale coherent motions (including Galactic shear and large-scale turbulent flows) that drive turbulent motions, and localized feedback from newborn stars that effectively counter self-gravity. The overall star formation rate is then relatively slow and inefficient at just a few percent conversion of gas to stars per local dynamical timescale across a wide range of densities (Krumholz & Tan 2007). However, the relative importance of the above processes for suppressing star formation is unknown, even for the case of our own Galaxy.

To investigate the star formation process within molecular clouds, a significant range of the internal structure of GMCs needs to be resolved including dense gas clumps expected to be the birth locations of star clusters. The global galaxy simula-

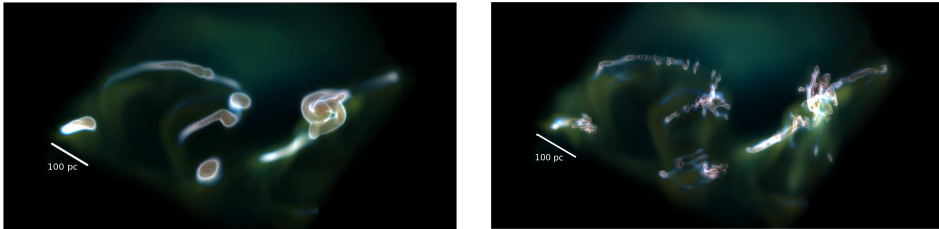


Figure 1. Volume rendering of the number density after 10 Myr for a uniform (left) and AMR (right) simulation with the same physics as TT09. “GMC” gas is coloured blue, while “Clump” gas is red. The white line shows a distance of 100 pc.

tions of Tasker & Tan (2009, hereafter TT09) followed the formation and evolution of thousands of GMCs in a Milky-Way-like disk with a flat rotation curve. However, with a spatial resolution of ~ 8 pc, only the general, global properties of the GMCs could be studied; not their internal structure. Following all of these GMCs to higher spatial resolution is very expensive in terms of computational resources. Therefore we need to use an alternative method.

Our approach is to extract a 1 kpc by 1 kpc patch of the disk, extending 1 kpc both above and below the midplane, centered at a radial distance of 4.25 kpc from the Galactic center. This is done at a time 250 Myr after the beginning of the TT09 simulation, when the disk has fragmented into a relatively stable population of GMCs. We then follow the evolution of the ISM, especially the GMCs, including their interactions, internal dynamics and star formation activity, down to clump-size, or parsec-size, scales. These local simulations are able to reach higher densities, resolve smaller mass scales and include extra physics compared to the global simulations.

The grid resolution of the initial conditions is $128^2 \times 256$ which corresponds to a cell size of 7.8 pc and serves as the root grid for the high resolution simulations. Most of the simulations we present here involve 4 levels of adaptive mesh refinement of the root grid, thus increasing the effective resolution to $2048^2 \times 4096$ or about 0.5 pc. Refinement of a cell occurs when the Jeans length drops below four cell widths, in accordance with the criteria suggested by Truelove et al. (1997) for resolving gravitational instabilities. The simulations performed in this paper were run using *Enzo* (e.g. O’Shea et al. 2004).

2. Resolving the GMCs

We first carry out the simulation with the physics and resolution identical to the global galaxy simulation of TT09, i.e. a grid resolution of ~ 8 pc and only the Rosen & Bregman (1995) cooling function down to 300K is included.

Figure 1 shows the gas density for this simulation (left panel) after 10 Myr. While the clouds show some signs of gravitational contraction, interaction and fragmentation over this time scale, they have not changed dramatically. In fact, the mass fraction of “GMC” gas (i.e. $n_{\text{H}} > 10^2 \text{ cm}^{-3}$) remains quite constant throughout the simulation, which spans a few free-fall times (Fig. 2). The volume fraction of “GMC” gas shows an initial decrease, but also remains relatively constant. Thus the clouds are roughly in virial equilibrium and this is reflected by the virial parameters of the clouds which are between 0.73 and 1.1 (Van Loo et al. 2012). The thermal pressure and non-thermal motions within the clouds provide enough support against self-gravity to prevent runaway

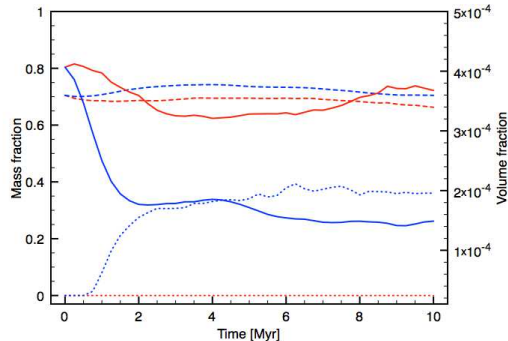


Figure 2. The mass fraction of gas in “GMCs” (dashed) and in “Clumps” (dotted) and the volume fraction of gas in “GMCs” (solid) for the uniform (red) and AMR model (blue).

gravitational collapse (even though the non-thermal motions are not well resolved in this uniform grid simulation). The nonthermal motions are continuously driven by bulk cloud motions in a shearing galactic disk as kinetic energy cascade down.

By increasing the resolution down to ~ 0.5 pc the GMCs can now be better resolved and the evolution of dense clumps within the clouds begins to be captured. While the mass fraction of “GMC” gas increases slightly, the volume fraction decreases by a factor of 2 within 2 Myr after which it remains roughly constant (see Fig. 2). In roughly the same time span, about half of the “GMC” gas accumulates in “Clumps” (i.e. $n_{\text{H}} > 10^5 \text{ cm}^{-3}$). Then the mass fraction in clumps remains nearly constant and reaches a new quasi-steady state. So, initially, the gas within the clouds collapses to form filaments with dense clumps due to the increased resolution (see right panel of Fig. 1). Concurrent with the contraction, the velocity dispersion in the clouds increases. The virial parameters of the clouds now lie between 1.6 and 4.5 (Van Loo et al. 2012). Non-thermal motions again counter the effects of self-gravity to virialise the cloud. The initial evolution of the clouds is thus a direct consequence of the increase in resolution.

3. Molecular cooling

While the increased resolution helps to describe the substructures of GMCs in greater detail, the thermal properties of the ISM are poorly reproduced. As only cooling is included in the simulations of the previous section, most of the gas within the disk is at the floor temperature of 300 K. To reproduce the multiphase character of the ISM, i.e. a cold, dense and a warm, diffuse phase, we include diffuse heating. Additionally, we study the influence of different cooling functions. While atomic cooling can be adequately described by the Rosen & Bregman cooling function, the Sanchez-Salcedo et al. (2002) function extends down to a temperature of 5 K, i.e. nearly two orders of magnitude lower, and includes a thermally unstable temperature range. To include molecular cooling, especially from H_2 and CO molecules, we adopt a novel approach. Using the simulation with the atomic cooling, the column extinction can be expressed as function of gas density. Such a one-to-one relation eliminates the need for time-consuming column-extinction calculations to assess the attenuation of the radiation field in the sim-

ulations. We also use this extinction-density relation to generate a table of cooling and heating rates as function of density and temperature with the code Cloudy (Ferland et al. 1998). More details on this approach are given in Van Loo et al. (2012).

Including diffuse heating mostly affects the gas outside the GMCs as this gas has a higher equilibrium temperature than 300 K (i.e. the temperature of the gas in the disk in the initial simulations). Then a higher external pressure acts as an additional force confining the GMCs. The higher external pressure resulting from this heating of the disk is, however, much smaller than the internal pressure of the GMCs, which is set by their self-gravitating weight.

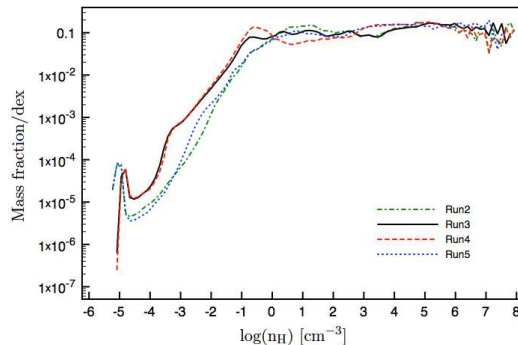


Figure 3. Mass-weighted Probability Density Function (PDF) for the Rosen & Bregman cooling with (Run 3) and without heating (Run 2), Sanchez-Salcedo et al. (Run 4) and Cloudy cooling function (Run 5) simulations after 10 Myr.

For the Sanchez-Salcedo et al. and Cloudy cooling function, the internal thermal pressure decreases by ~ 2 orders of magnitude (the floor temperature goes from 300K to 5K). However, the global properties of the clouds remain similar, e.g. the distribution of gas as function of density in these models is nearly identical (see Fig. 3). Thus, thermal pressure is negligible compared to self-gravity and turbulent pressure in setting the cloud properties. The PDFs also reveal that the clouds evolve to a state where a large fraction, 30-40% of the gas is in clumps. As in nearby GMCs this value is only between 0 and 15% (Eden et al. 2012), so there is a clear overproduction of dense clump gas in our simulations. The high clump formation efficiency is partly due to our resolution limit. We do not properly capture the formation of individual clumps so that the turbulent dissipation range is not fully resolved. The clumps then lack turbulent support against self-gravity hereby attaining higher densities and accumulating more mass.

4. Star formation

To model star formation, we allow collisionless star cluster particles, representing a *star cluster* of mass M_* , to form in the dense clumps of our simulations. These star cluster particles are created when the density within a cell exceeds a fiducial star formation threshold value of $n_{H,sf} = 10^5 \text{ cm}^{-3}$. We use a prescription of a fixed star formation efficiency per local free-fall time, ϵ_{ff} , for those regions with $n_H > n_{H,sf}$. Our fiducial

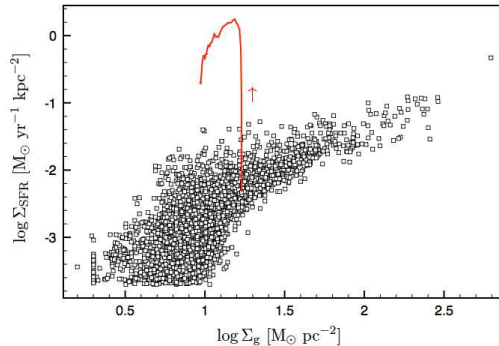


Figure 4. The star formation rate (Σ_{SFR}) as function of the gas surface density. The symbols show the observations of Bigiel et al. (2008), while the solid line shows the evolution of Σ_{SFR} in our simulation. The arrow shows the direction of the evolution.

choice of ϵ_{ff} is 0.02 as implied by observational studies (Zuckerman & Evans 1974; Krumholz & Tan 2007).

When a cell reaches the threshold density, a star cluster particle is created whose mass is calculated by

$$M_* = \epsilon_{\text{ff}} \frac{\rho \Delta x^3}{t_{\text{ff}}} \Delta t, \quad (1)$$

where ρ is the gas density, Δx^3 the cell volume, Δt the numerical time step, and t_{ff} the free-fall time of gas in the cell (evaluated as $t_{\text{ff}} = (3\pi/32G\rho)^{1/2}$). To avoid too many star particles of low mass, only star particles with a mass of $M_{*,\text{min}} = 100M_{\odot}$ are created with a probability of $M_*/M_{*,\text{min}}$. The motions of the star cluster particles are calculated as a collisionless N-body system within the total potential due to galaxy, gas and stars.

Star formation has not changed much of the global density structure or dynamics, but has reduced the maximum gas surface densities by about an order of magnitude compared to the model without star formation. As the star formation rate depends on the gas mass in dense clumps (Eq. 1), the evolution of the star formation rate follows the clump mass fraction. It is then not surprising that we find mean star formation rate of $0.8 M_{\odot} \text{ yr}^{-1} \text{ kpc}^{-2}$ over the 10 Myr time scale. The star formation rate in our simulations exceeds that expected from the Kennicutt-Schmidt relation (e.g. Bigiel et al. 2008) by \sim two orders of magnitude (see Fig. 4). This over efficiency of star formation in our simulations is a simple reflection of the high mass fraction in dense clumps.

5. Magnetic fields

Magnetic fields have been observed on large-scales in galaxies (Fletcher 2010) down to small-scales in dense cores (Girart et al. 2009). They provide additional support to the GMCs and can play a role in reducing the high clump mass fraction found in the hydrodynamical simulations.

To study the effect of magnetic fields, we ran MHD simulations where the initial conditions are threaded with a uniform magnetic field along the y -axis (i.e. the direction of the shear). The magnitude of the field varies between 1 and $10 \mu\text{G}$ rep-

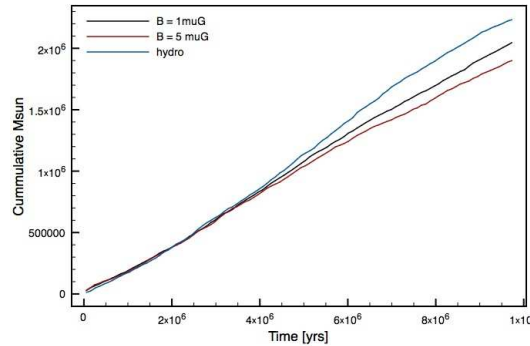


Figure 5. Cumulative mass in star particles for uniform HD and MHD simulations.

representing values around the mean Galactic value of $\sim 6\mu\text{G}$. The uniform simulations show slightly expanding clouds due to the additional support against self-gravity and less fragmentation with increasing magnetic field strength. When we include the star formation routine, albeit with a lower $n_{\text{H,sf}} = 10^2 \text{ cm}^{-3}$ and higher $M_* = 1000 M_\odot$, fewer star particles form in the MHD simulations than in the hydro simulations (see Fig. 5). However, to understand the impact of the field on clump formation, higher resolution simulations are required (and are currently in progress).

Acknowledgments. We thank Sam Skillman for the scripts to produce the rendered images. SvL acknowledges support from the SMA Postdoctoral Fellowship of the Smithsonian Astrophysical Observatory and JCT from NSF CAREER grant AST-0645412; NASA Astrophysics Theory and Fundamental Physics grant ATP09-0094; NASA Astrophysics Data Analysis Program ADAP10-0110. Resources supporting this work were provided by the NASA High-End Computing (HEC) Program through the NASA Advanced Supercomputing (NAS) Division at Ames Research Center.

References

- Bigiel, F., Leroy, A., Walter, F., et al. 2008, *AJ*, 136, 2846
 Eden, D. J., Moore, T. J. T., Plume, R., & Morgan, L. K. 2012, *MNRAS*, 2784
 Ferland, G. J., Korista, K.T. Verner, D.A. Ferguson, J.W. Kingdon, J.B. Verner, & E.M. 1998, *PASP*, 110, 761
 Fletcher, A. 2010, *Astronomical Society of the Pacific Conference Series*, 438, 197
 Girart, J. M., Beltrán, M. T., Zhang, Q., Rao, R., & Estalella, R. 2009, *Science*, 324, 1408
 Krumholz, M. R., & Tan, J. C., 2007, *ApJ*, 654, 304
 McKee, C. F., & Ostriker, J. C., 2007, *ARA&A*, 45, 565
 O’Shea, B. W., Bryan, G., Bordner, J., Norman, M. L., Abel, T., Harkness, R., & Kritsuk, A. 2004, *ArXiv Astrophysics e-prints*, astro-ph/0403044
 Rosen, A. & Bregman, J. N. 1995, *ApJ*, 440, 634
 Sánchez-Salcedo, F. J., Vázquez-Semadeni, E. & Gazol, A. 2002, *ApJ*, 577, 768
 Tasker, E. J., & Tan, J. C. 2009, *ApJ*, 700, 358
 Truelove, J. K., Klein, R. I., McKee, C. F., Holliman, J. H., Howell, L. H., & Greenough, J. A. 1997, *ApJ*, 489, L179
 Van Loo, S., Butler, M., & Tan, J. C., 2012, *ApJ*, submitted.
 Zuckerman, B., & Evans, N. J. II, 1974, *ApJ*, 192, L149